

Marquez et al., Sexual-dimorphism in human immune system aging.

Supplementary Figures.

Supplementary Figure 1. Age is the main driver of variation in PBMC genomic data.

Supplementary Figure 2. Shared and sex-specific epigenomic signatures of aging.

Supplementary Figure 3. Chromatin accessibility profiles for example loci.

Supplementary Figure 4. Shared and sex-specific transcriptomic signatures.

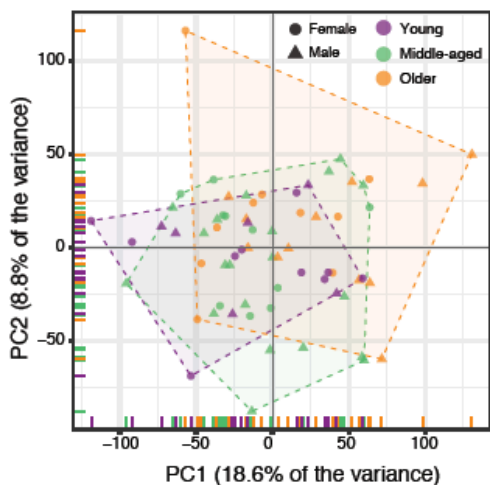
Supplementary Figure 5. Sex-dimorphic changes in monocyte- and B cell-associated loci.

Supplementary Figure 6. Epigenome and transcriptome changes over human adult lifespan.

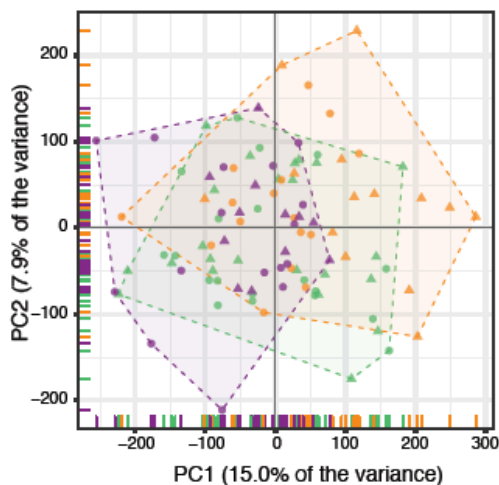
Supplementary Figure 7. Sex-specific patterns in temporal peaks/genes.

Supplementary Figure 8. Genomic differences between sexes at different ages.

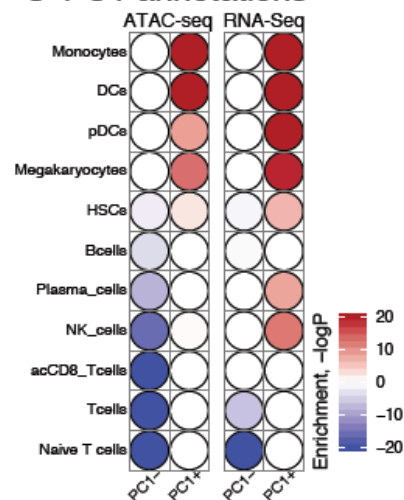
a PCA for RNA-seq data



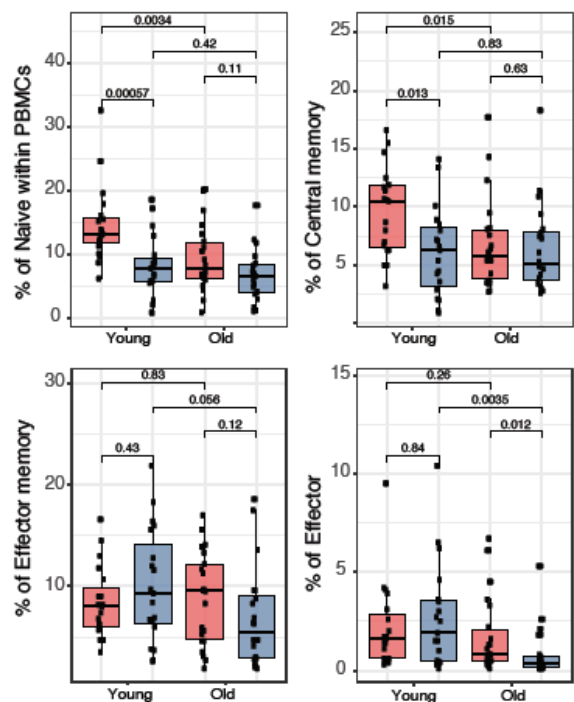
b PCA for ATAC-seq data



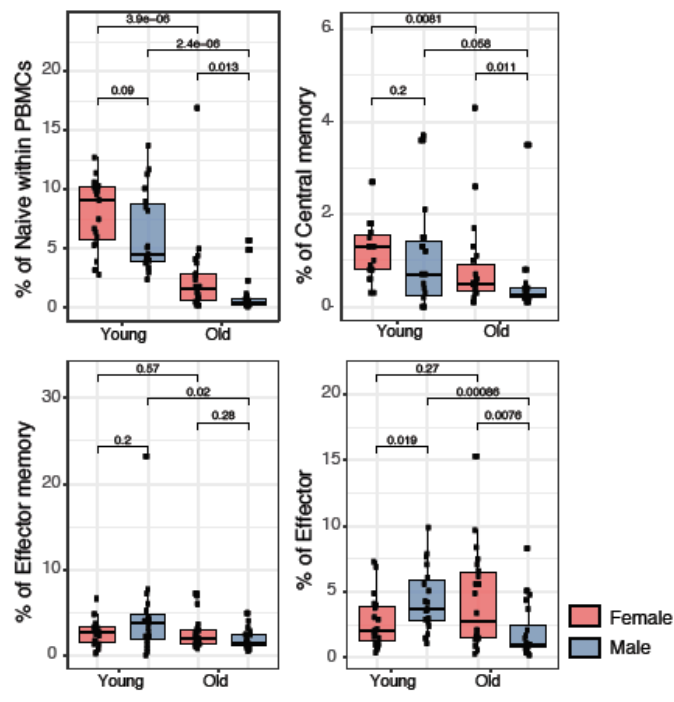
c PC1 annotations



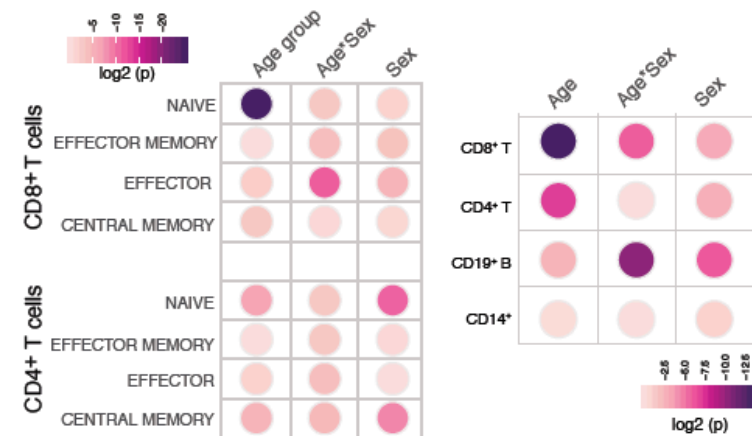
d Percent of CD4+ T cell subsets (n=80)



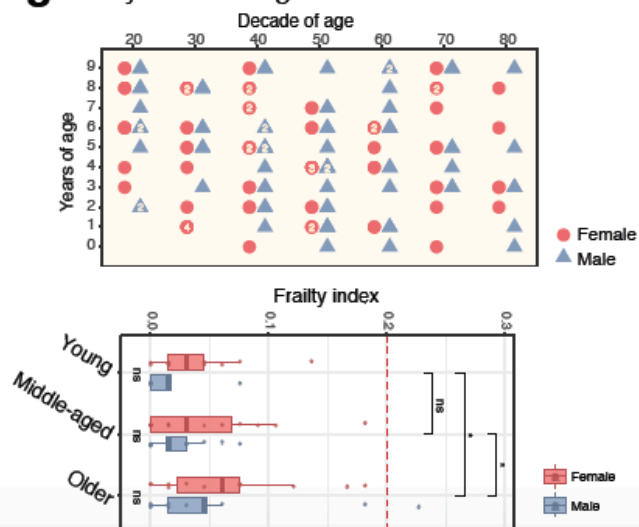
e Percent of CD8+ T cell subsets (n=80)



f Association of cell %s with age/sex

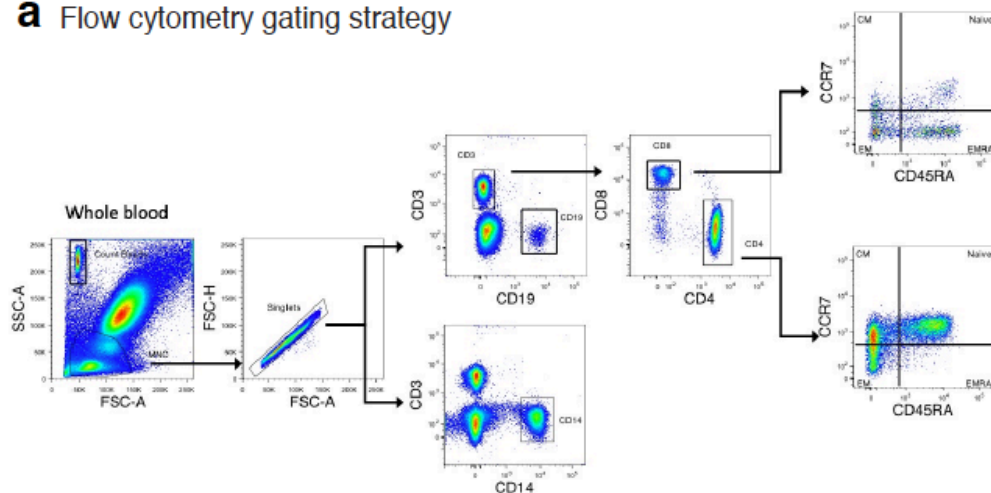


g Frailty index & age distribution

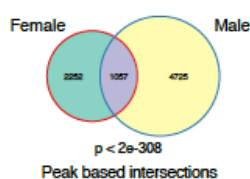


Supplementary Figure 1. Age is the main driver of variation in PBMC genomic data. Principal component analyses for (a) RNA-seq (n=74) and (b) ATAC-seq samples (n=100). PC1 explains 18.6% of variation in RNA-seq, 15% of variation in ATAC-seq data. (c) Functional enrichment of PC1-related genes using gene sets obtained from PBMC single-cell RNA-seq data. Marker genes are selected using PC1 scores that are $\geq 25^{\text{th}}$ percentile: top (positive) and bottom (negative). Genes with high and positive scores were enriched in myeloid cells (monocytes, DCs), whereas genes with high and negative scores were associated to adaptive cells, particularly naïve T cells. These enrichments align well with age-related increase in myeloid lineage and age-related decline in naïve T cell activity. Hypergeometric test is used to calculate enrichment p values. (d-e) Flow cytometry data (n= 80) reflect proportions of CD4⁺ (d) and CD8⁺ (e) T cell subsets within PBMCs. Subjects are stratified based on age groups and sex: Young: 22-40, Old: 65+ years old. Wilcoxon signed rank (two-sided) test is used to compare data from men and women, old and young subjects. Naïve CD4⁺ and CD8⁺ T cell proportions decline significantly with age in both sexes. (f) Significance values from generalized linear models (GLM) to establish the association between PBMC cell composition data with age group, sex, and their interaction (age*sex). Darker colors indicate stronger association. Age is strongly associated with the variation in naïve T cell proportions, whereas sex, age*sex is strongly associated with the variation in B cell proportions. (g) Top: Age of subjects spread comparable between sexes across decades. Bottom: Distribution of Rockwood frailty index (FI) values³⁹ stratified by age groups and sexes. No significant difference detected between sexes for age groups. The FI values increase with age, more so in women with none of the individuals having a value greater than 0.25. Most subjects were non-frail (FI: 0-0.1), a few were prefrail (FI >0.1-0.21) but regardless the frailty did not influence the observed genomic changes. Boxplots represent median, upper and lower quartiles. Source data are provided as a Source Data file for panels c, g.

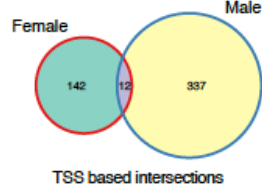
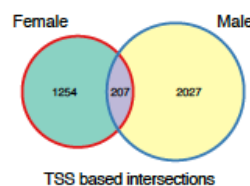
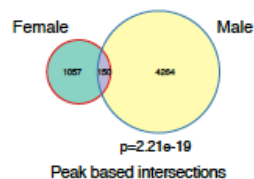
a Flow cytometry gating strategy



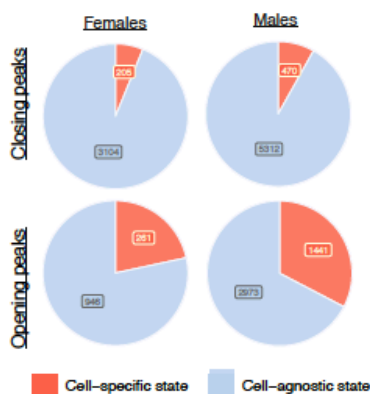
b Closing peaks



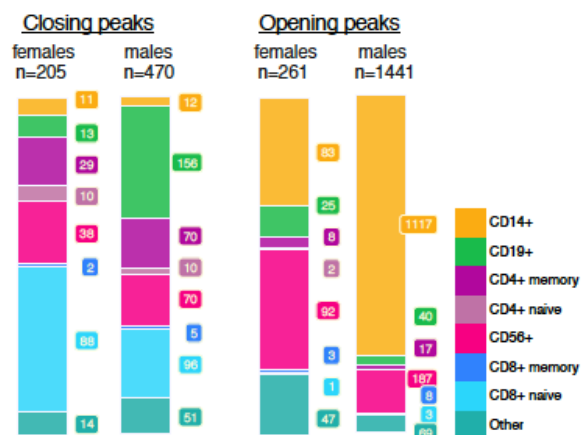
Opening peaks



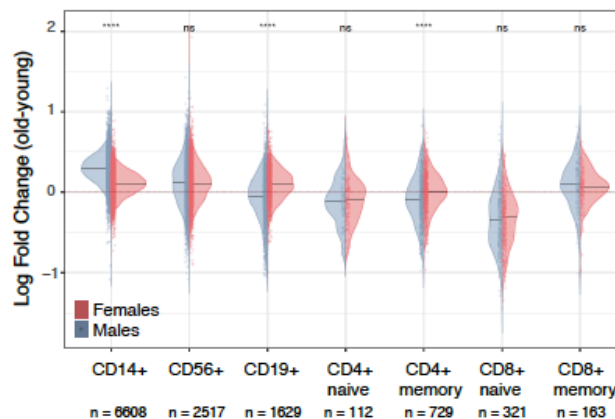
c Cell-specificity of DA peaks



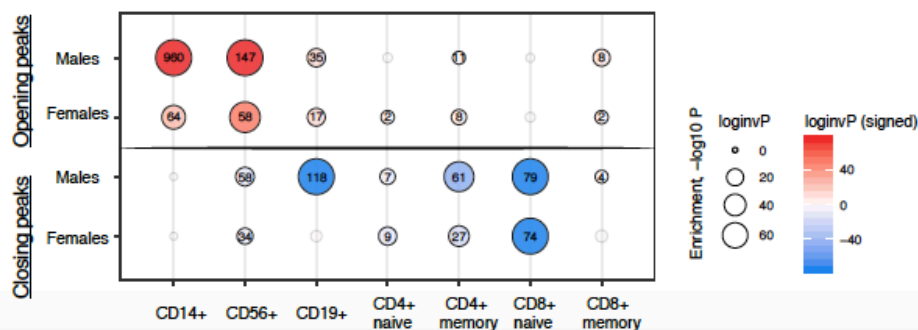
d Cell-specific ChromHMM REs



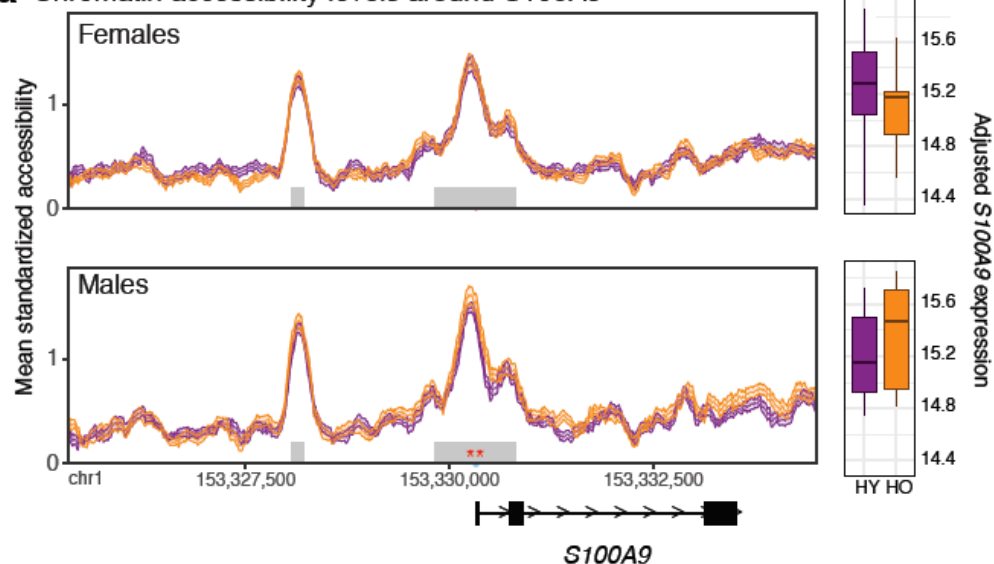
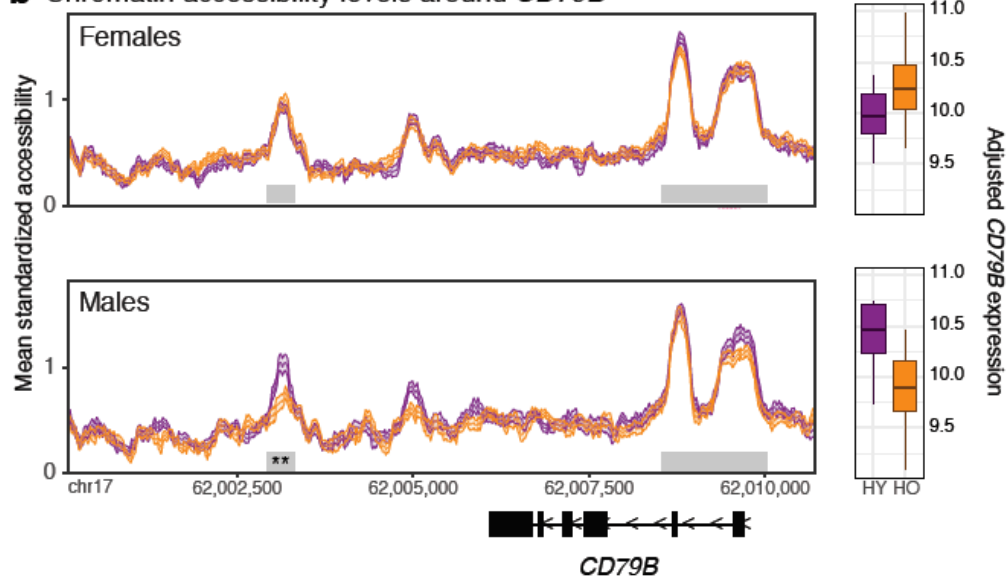
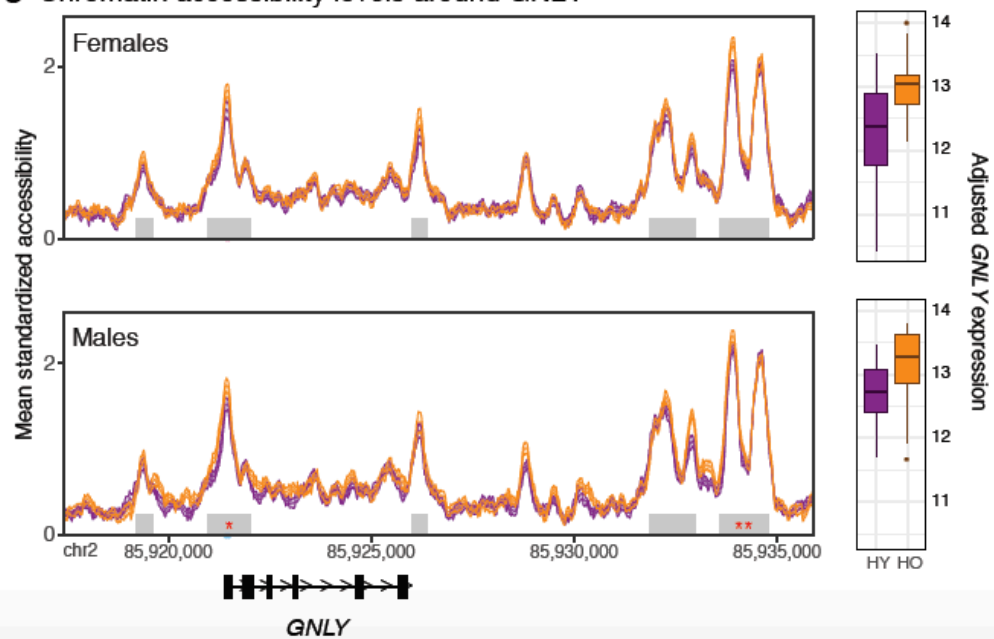
e Fold change distributions for cell-specific loci



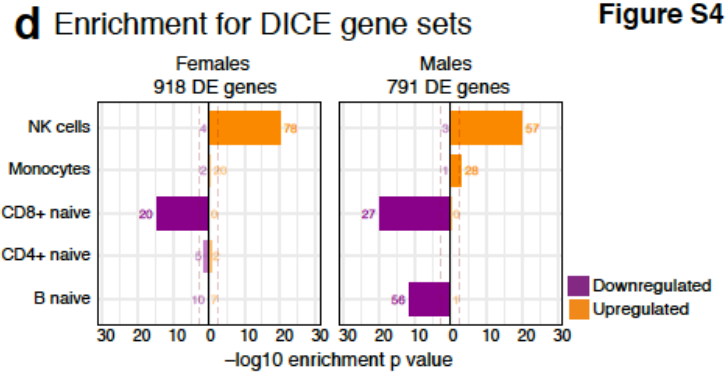
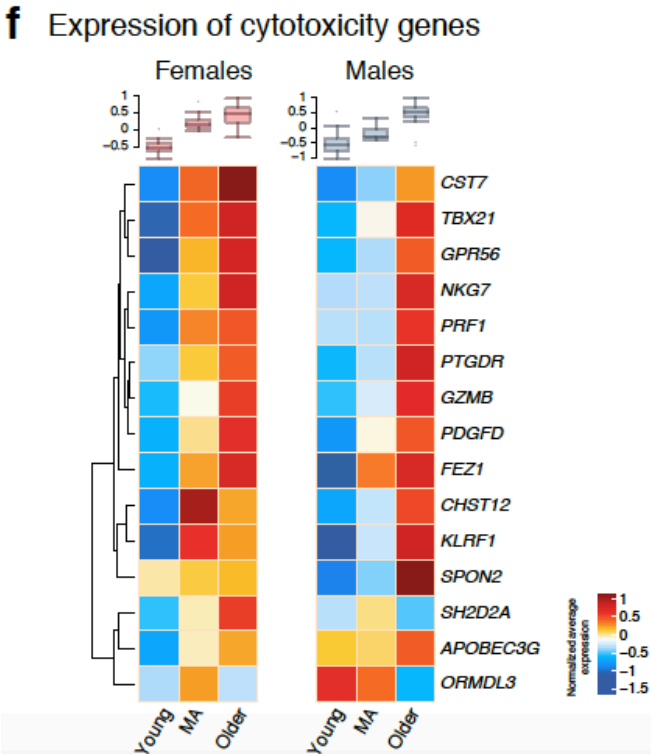
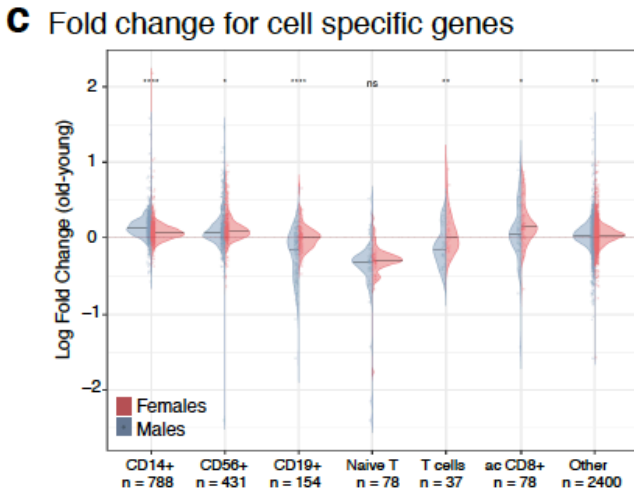
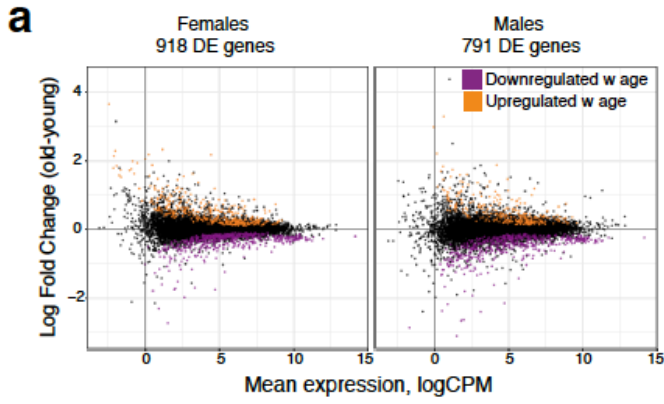
f Enrichment for cell-specific ChromHMM loci



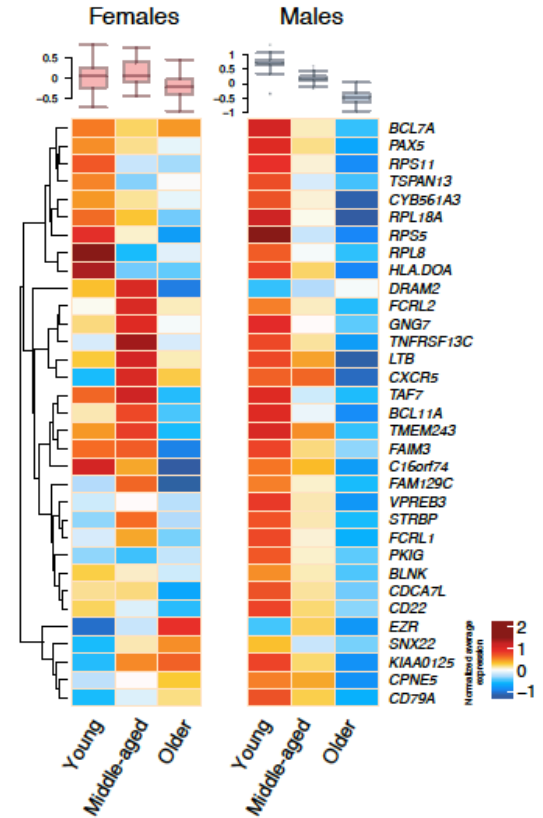
Supplementary Figure 2. Shared and sex-specific epigenomic signatures of aging. (a) Gating strategy used in flow cytometry data generation (b) Overlap between differentially accessible (DA) peaks (top) and genes associated to DA peaks (bottom) in women and men. Closing peaks overlap more between men and women. Note that the overlap is statistically significant for both opening and closing peaks based on Fisher's exact test for p-value calculations. (c) Distribution of cell-specific and cell-agnostic loci among DA peaks based on chromHMM states in PBMCs and immune cell subsets. Cell-specific regions are notably more common among opening peaks. (d) Number of cell-specific loci among closing/opening peaks in men and women. T and B cell-specific peaks are more prevalent among closing peaks, whereas NK and CD14⁺ monocyte specific peaks are more prevalent among opening peaks. (e) Fold change (old-young) distributions for chromatin accessibility levels at cell-specific loci. Biggest decrease is observed in naïve CD8⁺ T cell-specific loci in both men and women. Biggest increase is observed at CD14⁺ monocyte specific loci. The increase was much stronger in men. B cells specific loci on the average gain accessibility in women and lose accessibility in men with age. (f) Enrichment of cell-specific loci among DA peaks. Enrichment p values are calculated using hypergeometric test. Note the activation of innate cells (NK and monocytes) and inactivation of T cells with age. The enrichment p-values were more significant in men compared to women. B cell-specific regions were enriched for closing peaks in men and for opening peaks in women. Grayed out circles are non-significant at a 5% FDR; numbers on circles represent the number of peaks in each category. Source data are provided as a Source Data file for panels c, d, e, f.

a Chromatin accessibility levels around *S100A9***b** Chromatin accessibility levels around *CD79B***c** Chromatin accessibility levels around *GNLY*

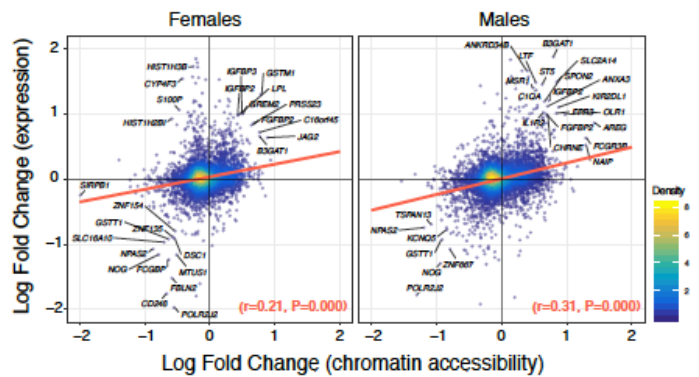
Supplementary Figure 3. Chromatin accessibility profiles for example loci. Left: Average chromatin accessibility profiles (grouped by age and sex) around *SI00A9* (a), *CD79B* (b), and *GPLY* (c) genes in women (top) and men (bottom). The peaks are denoted as gray bars and the ones that are statistically significantly different between young and old samples are marked with stars (red for opening peaks, black for closing peaks). Chromatin accessibility signals for each group includes averages as well as the confidence intervals for the group. Right: Normalized gene expression levels in young (HY) and older (HO) women (top) and men (bottom). HO= healthy old, HY=healthy young.



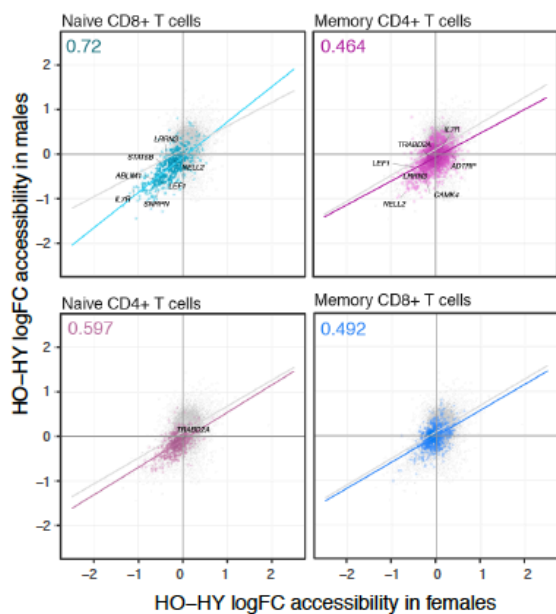
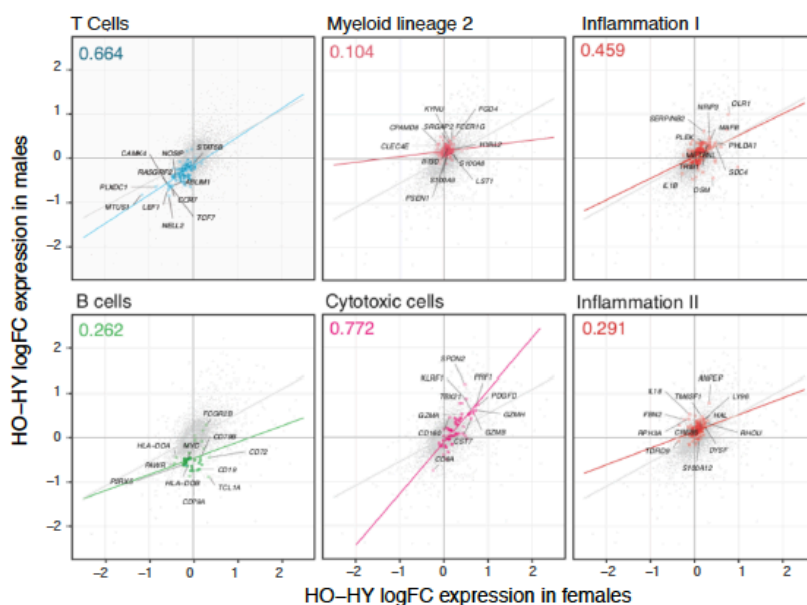
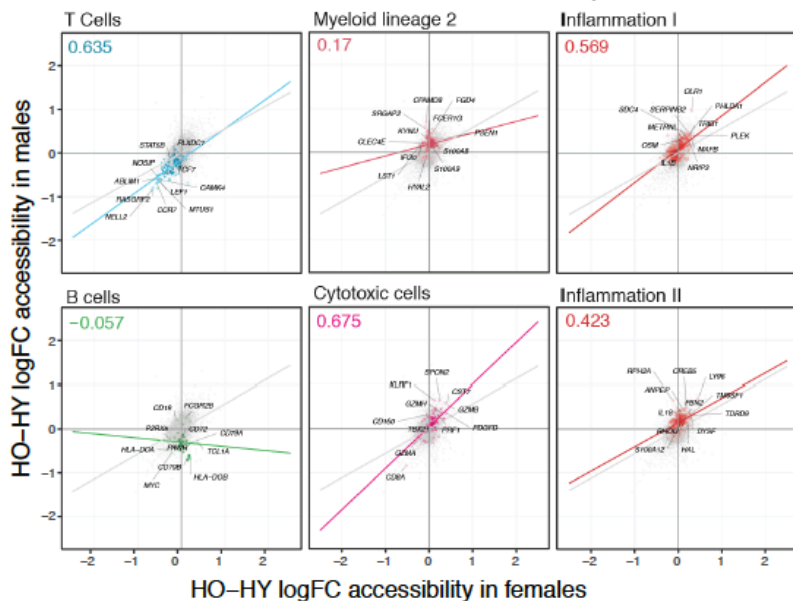
e Expression of B cell associated genes



g Correlation between ATAC-seq & RNA-seq

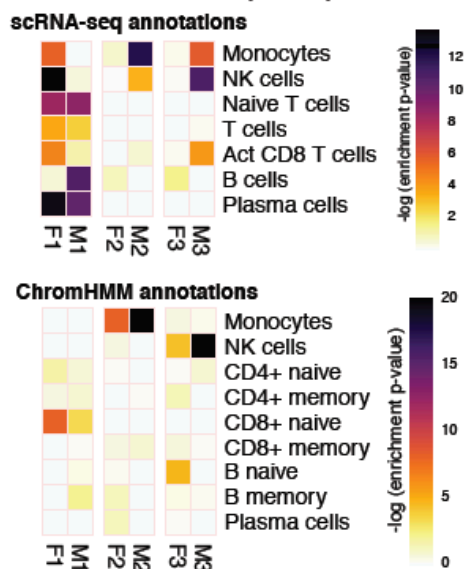


Supplementary Figure 4. Shared and sex-specific transcriptomic signatures. (a) MA plot representing log₂ fold change (older-young) versus average read count for RNA-seq data in women (left) and men (right). Differentially upregulated (downregulated) genes with age are represented in orange (purple). Differential gene expression was tested using a generalized linear model based on read counts, with significance assessed at a 10% FDR threshold, after using Benjamini-Hochberg P-value adjustment. (b) Overlap between differentially expressed (DE) genes in women and men. Note that despite sex differences, overlaps are statistically significant based on Fisher's exact test for p-value calculations. (c) Distribution of fold changes for gene expression levels of all cell-specific genes. Positive (negative) fold changes represent upregulation (downregulation) with age. CD14⁺ monocyte-specific genes are associated with positive fold change in both sexes, higher in men. B cell-specific genes are associated with negative fold changes only in men. (d) Enrichment of DE genes using cell-specific gene sets from the DICE database¹⁰. Naïve T cell genes are enriched in downregulated genes, NK cell genes are enriched in upregulated genes. B cell-specific genes are enriched in downregulated genes only in men. Enrichment p values were calculated using hypergeometric test. (e) Average normalized expression levels of B cell specific genes grouped by age group and sex. Box plots on the top summarize the data from all genes represented in the heatmap. (f) Average normalized expression levels of genes in the cytotoxic module grouped by age group and sex. Note the increase in cytotoxic molecules in both sexes. Box plots on the top summarize the data from all genes represented in the heatmap. (g) Correlation of age-related chromatin accessibility and gene expression changes based on chromatin accessibility at promoters in women (left) and in men (right). Color schema represent the density of points. Note that age-related remodeling ATAC-seq and RNA-seq data correlates positively and significantly in both sexes. R represents the correlation coefficient. Source data are provided as a Source Data file for panels a, c, d, g.

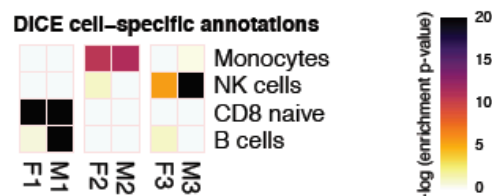
a ChromHMM annotations for ATAC-seq**b** Immune module annotations for RNA-seq**c** Immune module annotations for ATAC-seq

Supplementary Figure 5. Sex-dimorphic changes in monocyte- and B cell-associated loci. (a) Correlation of age-related ATAC-seq changes stratified by T cell subset specific loci from chromHMM states. Values at the top left corner represents the correlation coefficient between sexes only for the genes/loci associated to that cell type. (b-c) Correlation of age-related RNA-seq (b) and ATAC-seq (c) changes stratified by immune modules²². Values at the top left corner represents the correlation coefficient between sexes only for the genes/loci associated to that cell type/module. Source data are provided as a Source Data file for panels a, b, c.

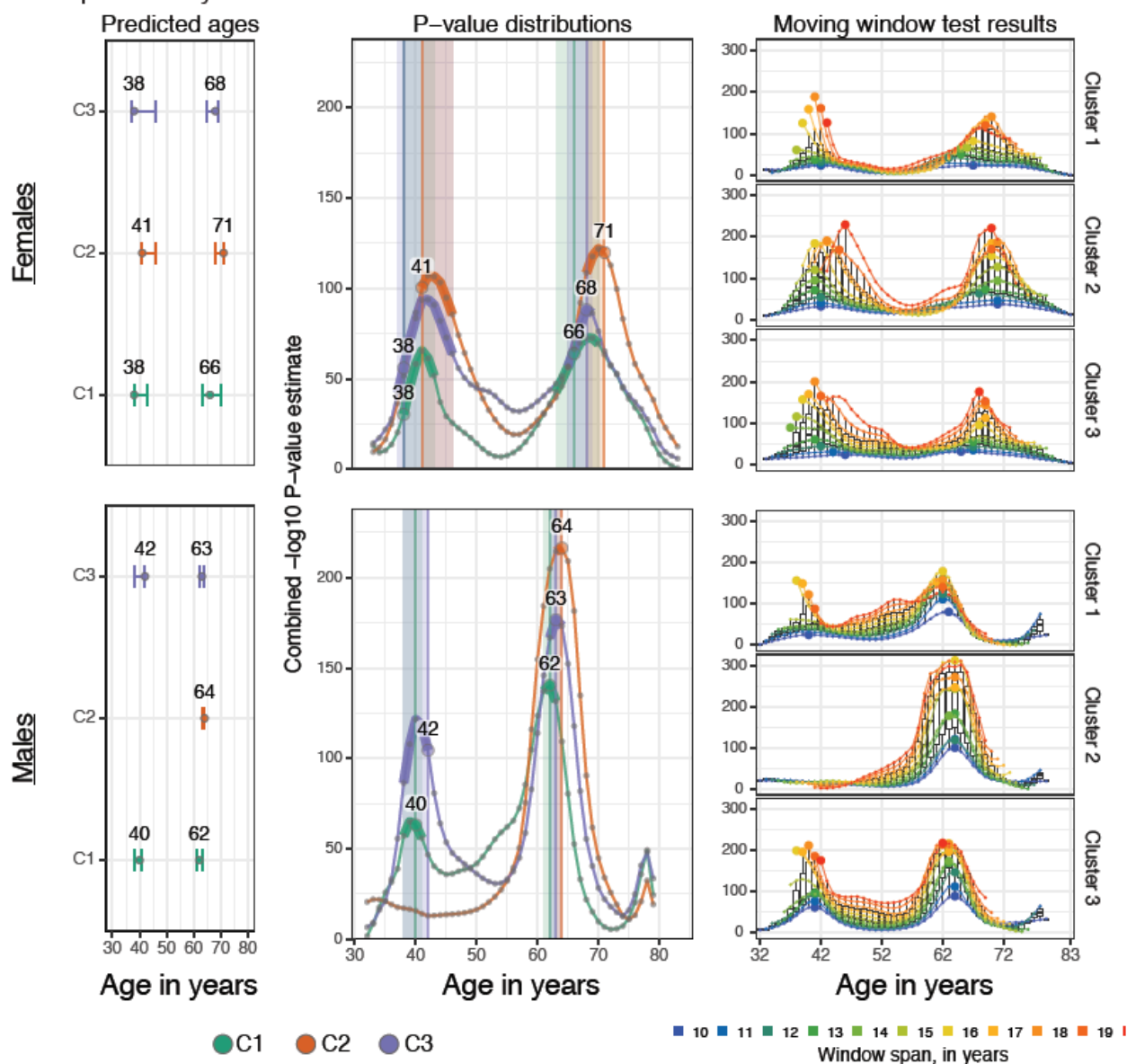
a Annotations of temporal peaks



b Annotations of temporal genes

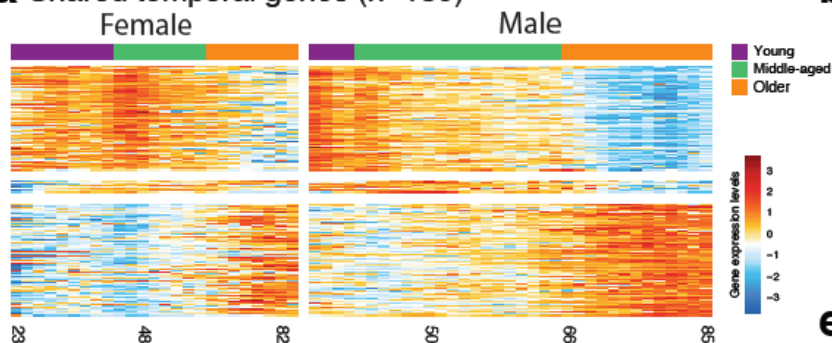


c Breakpoint analyses

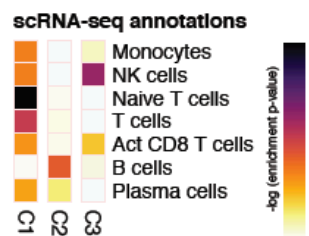


Supplementary Figure 6. Epigenome and transcriptome changes over human adult lifespan. (a) Annotations of temporal peaks using cell-specific expression (top) and chromatin states (bottom) in women (F1-F3) and in men (M1-M3). Colors represent hypergeometric enrichment test P-values. Single-cell RNA-seq-based enrichments based on nearest-gene annotations of temporal peaks. (b) Annotation of temporal genes using cell-specific gene sets from the DICE database¹⁰. (c) Detailed results from breakpoint analysis. Left: age range and median age of estimated breakpoints from each cluster in women (top) and men (bottom); Middle: $-\log(p\text{-value})$ of smoothed multi-scale moving window tests. Age range estimates for each cluster are represented as thickened curves and wide vertical bars; Right: $-\log(p\text{-value})$ of multi-scale analysis where each curve/color represents a distinct window span for the test, ranging from 10 to 20 years. Stronger evidence of a breakpoint emerges as the same age bracket is detected as significant at multiple window spans. C1, C2, C3 stands for cluster1-3. Source data are provided as a Source Data file for panels a, b.

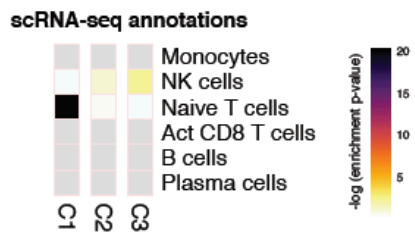
a Shared temporal genes (n=180)



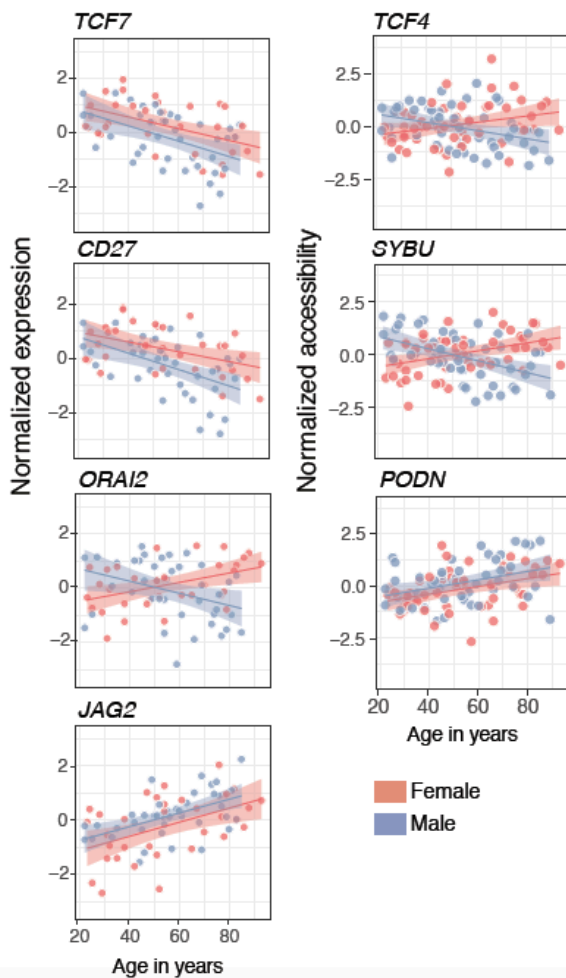
b Enrichment of common temporal peaks



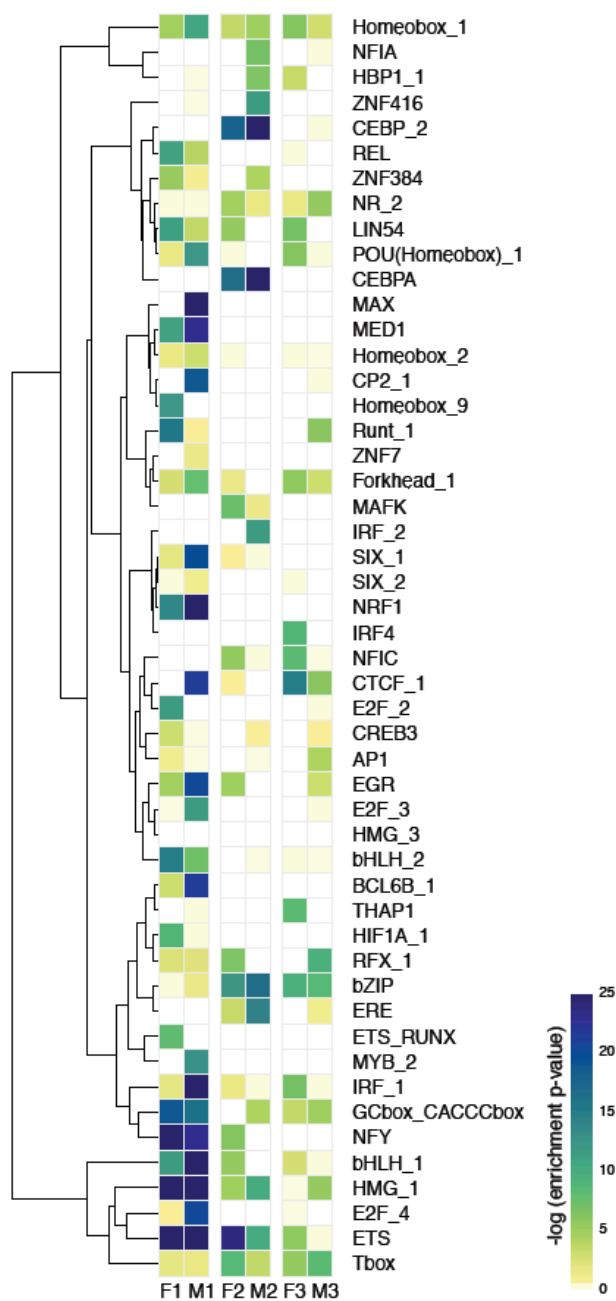
c Enrichment of common temporal genes



d Example temporal peaks/genes

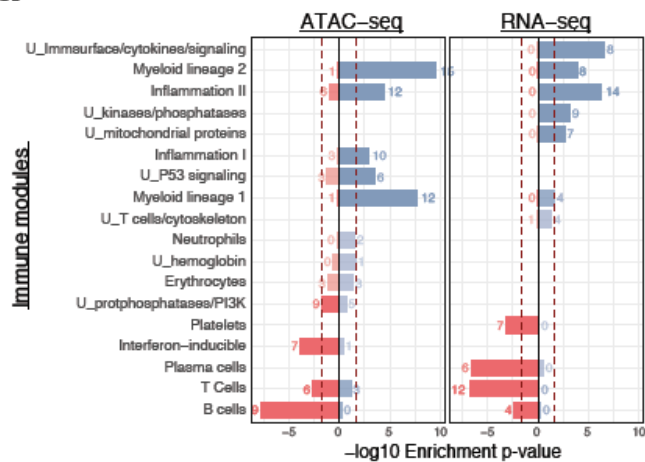


e TF enrichments for temporal peaks

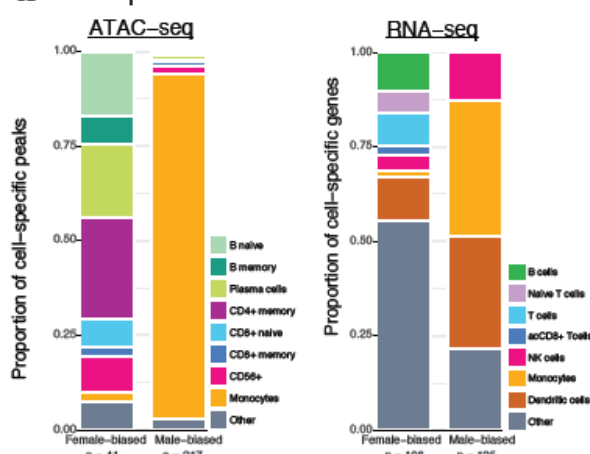


Supplementary Figure 7. Sex-specific patterns in temporal peaks/genes. (a) Heatmap of ARIMA-fitted expression values for genes with a significant chronological trend in both women and men (N=180). Values represent z score normalized gene expression values relative to the row mean. K-means clustering is used to group these peaks into three clusters (C1-C3) using concatenated data from men and women. Color bar on the top represents discrete age groupings as defined in this study (young, middle-aged, older). (b) Enrichment of cell-specific gene sets derived from scRNA-seq data among temporal clusters of OCRs, peaks are annotated to their nearest TSS. (c) Enrichment of cell-specific gene sets obtained from scRNA-seq among temporal and shared genes. Grey cells in plot indicate that there were insufficient genes in the gene sets to run an enrichment test. (d) Example temporal genes/peaks. (e) Transcription factor (TF) motif enrichment results for temporal peak clusters obtained separately from men and women. Peaks in each cluster is compared against the peaks in the other two clusters. Motif enrichment analyses carried out based on 1,388 PWMs, grouped into families based on the sequence similarity, and most significant p-value for each family is represented here. Source data are provided as a Source Data file for panels a, b, c.

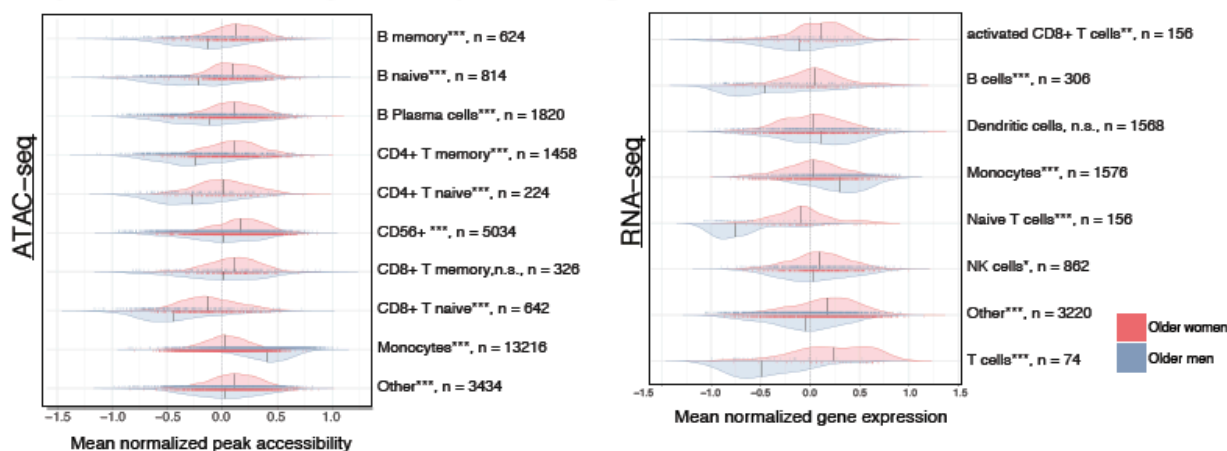
a Immune module annotations for sex-biased loci



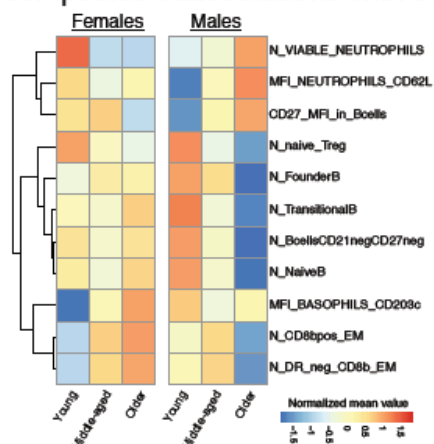
b Cell-specific loci annotations



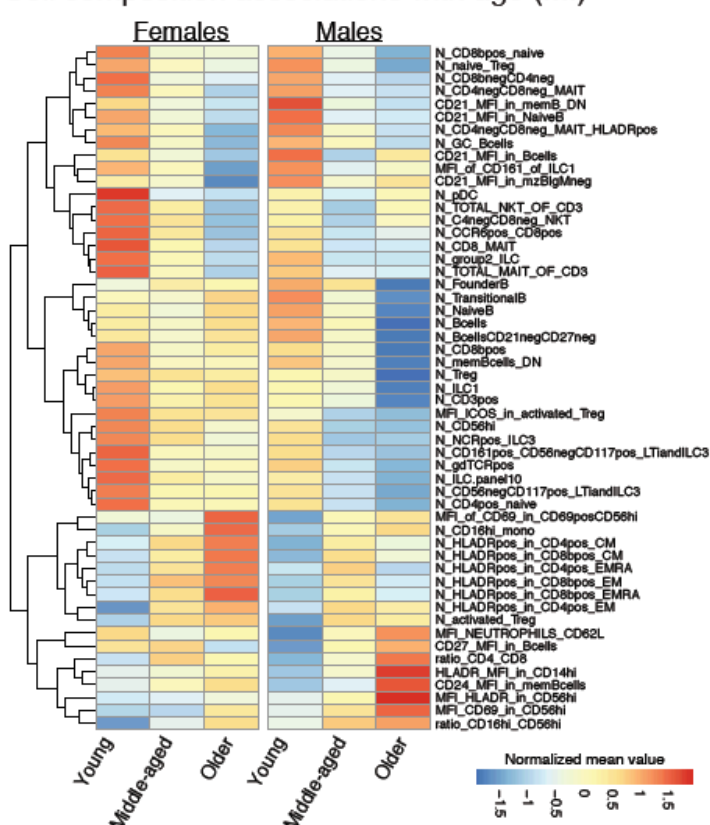
c Expression/accessibility of cell-specific loci/genes in older individuals



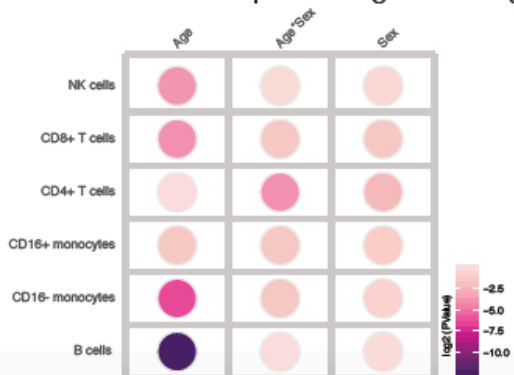
d Cell composition associations with sex (MI)



e Cell composition associations with age (MI)



f Association of cell percentages with age/sex



Supplementary Figure 8. Genomic differences between sexes at different ages. (a) Enrichment of sex-biased peaks/genes in older individuals using immune modules²². Note the male bias toward increased accessibility/expression for myeloid lineage and inflammation modules and the female bias toward T and B cell related modules. P-values are based on hypergeometric enrichment tests. Numbers on barplots represent the number of gene hits for each module. (b) Distribution of cell-specific loci among sex-biased peaks (left) and sex-biased genes (right). Note the enrichment of monocyte specific loci among male biased loci/genes. (c) Distribution of chromatin accessibility (left) and gene expression levels (right) in older men (blue) and older women (pink) for cell-specific genes. Stars next to the cell type name represent whether there is a significant difference between distributions in men and women. N represents the total number of cell-specific loci/genes used in each analysis. (d) Flow cytometry data from Milieu Intérieur Consortium¹² (n=892) re-analyzed using generalized linear models (GLMs) to associate cell counts or MFI values to sex. Rows represent the measurements that has been significantly associated to sex (FDR 5%). Values in heatmap represent the average value across individuals stratified based on sex and age group. Note the male-specific decline in different B cell populations after 65 years old, in agreement with our cohort. (e) Flow cytometry data from Milieu Intérieur Consortium¹² (n=892) re-analyzed using generalized linear models (GLMs) to associate cell counts or MFI values to age. Rows represent the measurements that has been significantly associated to age (FDR 5%). Values in heatmap represent the average value across individuals stratified based on sex and age group. (f) Mass cytometry data from Whiting *et. al.*²⁹ re-analyzed using linear models to associate cell percentages to age and sex. Colors represent the association p-value. Note that B cells are the most significantly associated to age in this cohort. Source data are provided as a Source Data file for panels a, b, c.